
GAN-BASED FEDERATED LEARNING FOR LABEL PROTECTION IN BINARY CLASSIFICATION

Yujin Han
Department of Biostatistics
Yale University
CT 06520, USA
yujin.han@yale.edu

Leying Guan*
Department of Biostatistics
Yale University
CT 06520, USA
leying.guan@yale.edu

October 3, 2024

ABSTRACT

As an emerging technique, vertical federated learning collaborates with different data sources to jointly train a machine learning model without data exchange. However, federated learning is computationally expensive and inefficient in modeling due to complex encryption algorithms and secure computation protocols. Split learning offers an alternative solution to circumvent these challenges. Despite this, vanilla split learning still suffers privacy leakage. Here, we propose the Generative Adversarial Federated Model (GAFM), which integrates the vanilla split learning framework with the Generative Adversarial Network (GAN) for protection against label leakage from gradients in binary classification tasks. We compare our proposal to existing models, including Marvell, Max Norm, and SplitNN, on three publicly available datasets, where GAFM shows significant improvement regarding the trade-off between classification accuracy and label privacy protection. We also provide heuristic justification for why GAFM can improve over baselines and demonstrate that GAFM offers label protection through gradient perturbation compared to SplitNN.

1 Introduction

Federated learning trains an algorithm across multiple decentralized remote devices or siloed data centers without exchanging their local data. Depending on different data partitioning methods, federated learning can be divided into three categories. They are horizontal federated learning (HFL), vertical federated learning (VFL), and federated transfer learning Yang et al. (2019). In VFL, the data is vertically partitioned, and local participants own datasets that share the same sample space but differ in feature space Hardy et al. (2017). With progressively stricter regulation of data privacy by government institutions such as the CCPA1 Pardau (2018) and GDPR3 Voigt & Von dem Bussche (2017), VFL is considered an effective solution for encouraging enterprise-level data collaborations, as it enables both collaboratively training and privacy protection. However, there are some concerns about VFL. One of these is the huge overhead in memory costs and processing time. To provide a strong privacy guarantee for cross-silo training, VFL performs complex cryptographic operations, such as additive homomorphic encryption Hardy et al. (2017) and secure multi-party computation Mohassel & Zhang (2017), which are extremely expensive to compute. It has been reported that 80% of the training time of the deep learning-based federated learning is on encryption and decryption Zhang et al. (2020).

Vertical split learning was proposed to solve this problem Gupta & Raskar (2018); Vepakomma et al. (2018); Abuadbbba et al. (2020); Ceballos et al. (2020). In vertical split learning, each participant (passive party) trains a partial model locally and then aggregates all outputs before feeding them to the server (active party). The active and passive parties then collaboratively train all participants' local models through back-propagation. Split learning allows multiple participants to jointly train a federated model without encryption of intermediate results (intermediate computations of the cut layer), thus reducing the computation expense. SplitNN applies the idea of split learning to neural networks and has been used to analyze healthcare data (Poirot et al., 2019; Ha et al., 2021).

*Corresponding author

In VFL, we want to guard against both label leakage from gradients (LLG) (Wainakh et al., 2022) and passive party’s feature leakage (Aono et al., 2017; Luo et al., 2021). In other words, we care not only about how much the active party can infer about the passive parties’ features but also how much the honest-but-curious adversary can infer about the active party’s label through the gradient as we train the model. Despite their strengths, vanilla split learning approaches, including SplitNN, still face the privacy information leakage issue. The security of split learning relies on the assumption that neural networks are black boxes and the attacker cannot recover the data and label information from the intermediate computations. Such an assumption does not necessarily hold, with intermediate gradient information flowing from the active party to the passive party exposing the feature information and the label information (Erdogan et al., 2021; Zhu et al., 2019). Previously, researchers have tried to provide security for SplitNN (Ceballos et al., 2020; Erdogan et al., 2021; Titcombe et al., 2021; Pereteanu et al., 2022), but they only focus on how to protect the passive party’s feature privacy from being stolen by the active party, while neglecting the risk of exposure to the highly sensitive information contained in labels.

Here, we propose a Generative Adversarial Federated Model (GAFM), which protects against LLG by combining SplitNN with generative adversarial networks (GANs) (Goodfellow et al., 2014). We reinterpret SplitNN from the generative adversarial perspective and view the task for each passive party as learning the generator’s input using their local data. And the prediction distribution generated by the generator should be close to the response distribution held by the active party. The proposed GAFM framework offers better protection against LLG without sacrificing much prediction accuracy compared to existing methods. In this paper, we focus on applying GAFM to the binary classification problem, which is prevalent in areas such as healthcare and finance.

The paper is organized as follows. We summarize related work in section 2. In section 3, we present the GAFM model and its algorithm, where we also provide heuristic justification for why GAFM protects against LLG compared to SplitNN and demonstrate that GAFM outputs more mixed intermediate gradients to protect the label privacy. We then conduct numerical experiments comparing GAFM with competing methods on three publicly available datasets in section 4.

2 Related Work

SplitNN-driven Vertical Partitioning Model. SplitNN allows multiple participants to have the same batch of samples but different features and to learn the same distributed model without sharing data Gupta & Raskar (2018); Vepakomma et al. (2018); Ceballos et al. (2020). In SplitNN, each passive party trains a partial neural network locally. The layer at which the active and passive parties share information (gradients from the active party and prediction from the passive parties) is called the cut layer. At the cut layer of SplitNN, each participant trains a fixed portion of the neural network locally and passes the intermediate results to the active party. The active party then aggregates intermediate results and implements backward propagation to update the local parameter of each participant. There are various aggregation methods, such as element-wise average, element-wise maximum, element-wise sum, element-wise multiplication, concatenation, or non-linear transformation (Ceballos et al., 2020).

Label protection via random gradient perturbation. To alleviate label information leakage through intermediate gradients at the cut layer, one solution is adding randomness to the intermediate gradients which have been used in HFL (Abadi et al., 2016; Geyer et al., 2017; Hu et al., 2020). **Marvell** (Li et al., 2021) is a random perturbation technique and can be applied to binary classification problems. Marvell protects the label privacy by perturbing the intermediate gradients. It aims to find the optimal zero-centered Gaussian perturbations to minimize the sum of KL divergences between the two perturbed distributions, under a budget constraint on the amount of perturbation added:

$$\begin{aligned} \min_{W^{(0)}, W^{(1)}} \quad & \text{KL}(\tilde{P}^1 \| \tilde{P}^0) + \text{KL}(\tilde{P}^0 \| \tilde{P}^1) \\ \text{s.t.} \quad & \alpha \text{tr}(\Sigma_0) + (1 - \alpha) \text{tr}(\Sigma_1) \leq C, \end{aligned} \quad (1)$$

where $W^{(k)} = \mathcal{N}(0, \Sigma_k)$, $k = 0, 1$, are the Gaussian perturbations added to class 0 and class 1, \tilde{P}^k is the distribution of perturbed intermediate gradients from k after convolution with the Gaussian noise $W^{(k)}$ for $k = 0, 1$, and C is the budget for how much random perturbation Marvell is allowed to add. As the intermediate gradients with different labels become less distinguishable, intuitively, the difficulty for attackers to infer labels from gradients also increases.

Max Norm (Li et al., 2021) is an improved heuristic approach of adding zero-mean Gaussian noise with non-isotropic and example-dependent covariance. More concretely, for the intermediate gradient g_j of data point j , Max Norm adds the zero-mean Gaussian noise η_j to it with the covariance as

$$\sigma_j = \sqrt{\frac{\|g_{max}\|_2^2}{\|g_j\|_2^2} - 1}, \quad (2)$$

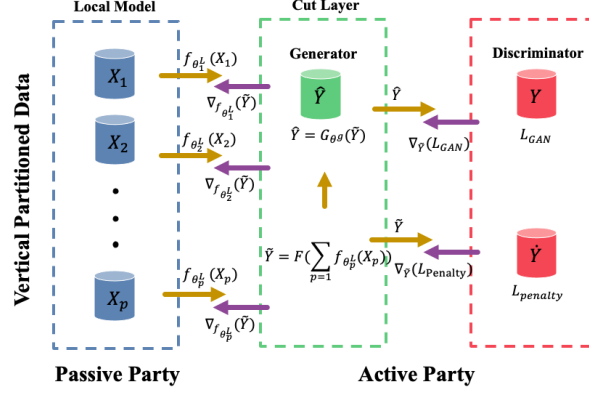


Figure 1: Systemic Structure of Generative Adversarial Federated Model.

where $\|g_{max}\|_2^2$ is the largest squared 2-norm in a batch. Max Norm is a simple, straightforward, and parameter-free perturbation method. But it does not have strong theoretical motivation and cannot guarantee to defend unknown attacks.

Generative Adversarial Networks. The Generative Adversarial Network (GAN) trains both a discriminator D and a generator G . Sampling from a uniform or Gaussian distribution as the input variable Z , generator G maps Z to the data space. The discriminator D aims to identify whether the distribution is from the real data or from the generated data. D and G continuously play a zero-sum game until convergence. For example, with cross-entropy loss, GAN considers the following optimization problem (Goodfellow et al., 2014):

$$\min_G \max_D L_{GAN}(G, D) = E_X[\log(D(X))] + E_Z[\log(1 - D(G(Z)))]. \quad (3)$$

GAN In Federated Learning. Previously, researchers have combined GAN and HFL for different purposes. In HFL, there are multiple clients who can access the same set of features and responses for different samples. GAN has been studied in this setting in three directions: (1) generating malicious attacks (Hitaj et al., 2017; Wang et al., 2019), (2) training high-quality GAN across distributed data under, e.g., privacy, constraints Hardy et al. (2019); Rasouli et al. (2020); Mugunthan et al. (2021), and also recently, (3) privacy protection of client data Wu et al. (2021). In FedCG, the authors let each client train a classifier predicting the response Y using Z extracted from the original feature X , and a conditional GAN that learns the conditional distribution of Z given Y . The classifiers and generators (instead of the extracted Z) from different clients are then passed to the server for updating the common model. It has been shown that FedCG can effectively protect clients' data privacy. These previous works have demonstrated a promising role of GAN in HFL, but we are not aware of any prior work investigating the GAN model for label protection in VFL.

3 Generative Adversarial Federated Model

3.1 Generative Adversarial Federated Model (GAFM)

In this section, we describe the Generative Adversarial Federated Model (GAFM), which enhances label privacy protection against LLG without sacrificing much prediction accuracy compared to the vanilla splitNN pipeline. Fig.1 demonstrates the model structure of GAFM.

Given the local model $f_{\theta_p^L}$, the passive party p in GAFM passes the intermediate results $\tilde{Y}_p = f_{\theta_p^L}(X_p)$ to the active party, which is aggregated through $\tilde{Y} = F(\sum_p \tilde{Y}_p)$. And $F(\cdot)$ is a known transformation function, e.g., the identity function. The GAFM loss consists of two parts. The first part is a GAN loss L_{GAN} defined in (4), which quantifies the distance between the distribution of $\hat{Y} = G_{\theta_g}(\tilde{Y})$ and the distribution of Y using Wasserstein-1 distance or Earth-Mover distance (Arjovsky et al., 2017):

$$L_{GAN}(\theta^d, \theta^g; \varepsilon) = E_Y [D_{\theta^d}(Y + \varepsilon)] - E_X [D_{\theta^d}(G_{\theta^g}(\tilde{Y}))], \quad (4)$$

where $\varepsilon \sim N(0, \sigma^2)$ is a small additive Gaussian noise so that $Y + \varepsilon$ has a continuous support. The Wasserstein loss encourages the predicted distribution to be similar to that of the empirical response and is applicable to multi-class classification tasks (Frogner et al., 2015). The parameters θ^d represent model parameters for the discriminator, and θ^g are model parameters of the generator. That is, the P passive parties locally train P models based on their own data, and their outputs are aggregated as the input \tilde{Y} to the generator. Then the final prediction is $\hat{Y} = G_{\theta^g}(\tilde{Y}) = G_{\theta^g}(F(\sum_p (f_{\theta_p^L}(X_p)))$ which is obtained through the generator.

The second part is the penalty loss $L_{penalty}$ that encourages the two classes to be separated and is defined in (5) which measures the distance between intermediate results \tilde{Y} and the randomized response \dot{Y} :

$$L_{penalty}(\theta_p^L; u) = -E_{XY}[\dot{Y} \log(\tilde{Y}) + (1 - \dot{Y}) \log(1 - \tilde{Y})]. \quad (5)$$

We define $(\dot{Y}|Y = 1) = 0.5 + u$ and $(\dot{Y}|Y = 0) = 0.5 - u$ where $u \sim \text{Uniform}(0, \Delta)$ and $\Delta \in [0, 0.5]$. We use the randomized \dot{Y} instead of the original response Y to improve label protection against LLG. When $\Delta = 0$, no label information from original data is used, and when $\Delta > 0$, the randomized pseudo-response \dot{Y} guides the classifier while avoiding excessive label leakage from the penalty loss, which happens when using Y as shown by previous work Li et al. (2021).

The final GAFM loss combines L_{GAN} and $L_{penalty}$, and is defined below in (6),

$$\min_{\theta^g, \theta_p^L} \max_{\theta^d} L_{GAFM}(\theta^d, \theta^g, \theta_p^L) = L_{GAN}(\theta^d, \theta^g; \varepsilon) + \gamma L_{penalty}(\theta_p^L; u), \quad (6)$$

where $\gamma > 0$ is a hyper-parameter.

Algorithm 1: Generative Adversarial Federated Model

Input : Training data $X_1, X_2, \dots, X_P \in \mathbb{R}^{n \times d}$, training labels $Y \in \mathbb{R}^n$, sample $u \sim \text{Uniform}(0, \Delta)$, $\varepsilon \sim N(0, \sigma^2)$, epoch T , learning rates $\alpha^d, \alpha^g, \alpha^L$ and clip value c

```

1 Initialize  $\tilde{Y}_1^0, \tilde{Y}_2^0, \dots, \tilde{Y}_P^0$  from a Uniform or Gaussian distribution to get  $\tilde{Y}^0$  and initialize  $\theta_d^0, \theta_g^0$  and  $\theta_L^0$ 
2 while Not converge do
3   Active party
4   /* Step 1: Update the discriminator */
5   The active party computes the prediction  $\hat{Y} \leftarrow G_{\theta^g}(\tilde{Y})$  and updates the discriminator by
      $\theta^d \leftarrow \theta^d + \alpha^d \nabla_{\theta^d} L_{GAN}$  and clip  $\theta^d \leftarrow \text{clip}(\theta^d, -c, c)$ .
6   /* Step 2: Update the generator */
7   Then the active party updates the generator by  $\theta^g \leftarrow \theta^g - \alpha^g \nabla_{\theta^g} L_{GAN}$ .
8   /* Step 3: Back-propagation */
9   The active party back propagates normalized gradients with respect to  $\tilde{Y}$  to the passive parties
      $\text{grad}_{\tilde{Y}} = f_{Norm}(\nabla_{\tilde{Y}} L_{GAN}) + \lambda f_{Norm}(\nabla_{\tilde{Y}} L_{Penalty})$ , where  $f_{Norm}$  is a normalization operation defined in
     (8).
10  Passive parties
11  for  $p = 1, \dots, P$  do
12    /* Step 4: Update local models */
13    Based on the locally determined model architecture and  $\text{grad}_{\tilde{Y}}$ , passive party  $p$  trains the local model and
      updates  $\theta_p^L$ .
14    /* Step 5: Forward-propagation */
15    Then, update  $\tilde{Y}_p \leftarrow f_{\theta_p^L}(X_p)$ .
16  end
17 end
```

The model parameters $\theta^g, \theta^d, \theta_p^L$ are updated sequentially:

- (1) Update θ^d to maximize the GAN loss $\theta^d \leftarrow \arg \max_{\theta^d} L_{GAN}(\theta^d, \theta^g; \varepsilon)$ given θ^g, θ_p^L .
- (2) Update θ^g to minimize the GAN loss $\theta^g \leftarrow \arg \min_{\theta^g} L_{GAN}(\theta^d, \theta^g; \varepsilon)$ given θ^d, θ_p^L .

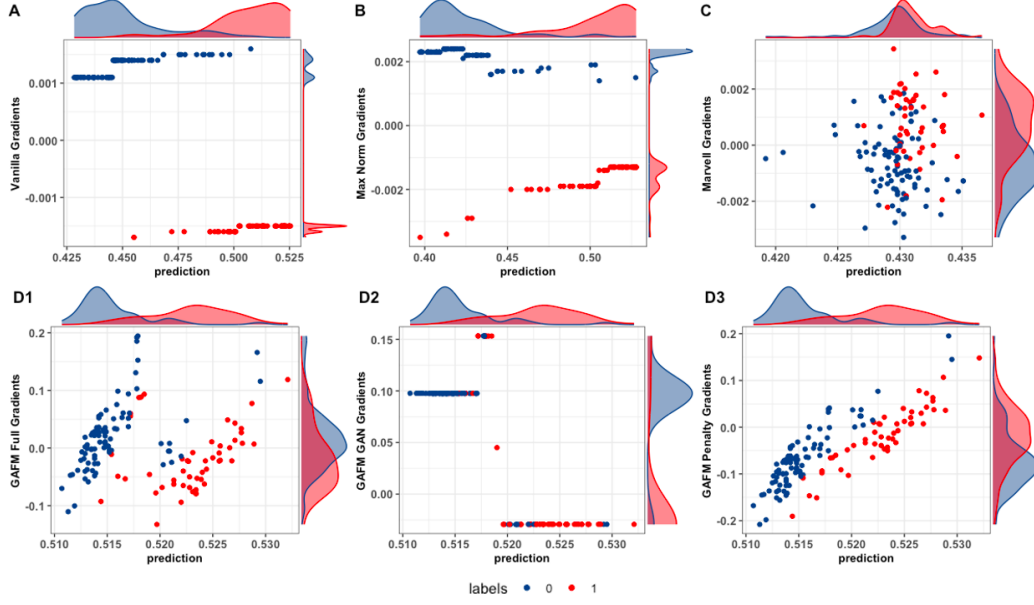


Figure 2: Prediction \hat{Y} vs. Intermediate Gradients of different models on Spambase. Fig.2 D1 is the full gradients of GAFM (gradients from L_{GAFM}) with $\Delta = 0.05$ which is much more mixed compared to that of Vanilla and Max Norm. Fig.2 D2 is gradients from L_{GAN} and Fig.2 D3 is gradients from $L_{penalty}$. The differences in gradient class centers from L_{GAN} and $L_{penalty}$ are in opposite direction, leading to mutual cancellation when forming the gradient for L_{GAFM} .

(3) Update θ_p^L to minimize the GAFM loss $\theta_p^L \leftarrow \arg \min_{\theta_p^L} L_{GAFM}(\theta^d, \theta^g, \theta_p^L; \varepsilon, u)$ given θ^d, θ^g .

The final algorithm implements the above procedures via the Adam optimizer with learning rates α^d , α^g and α_p^L respectively. Algorithm 1 provides the details.

3.2 Can GAFM protect against LLG?

We demonstrate that GAFM can provide better protection against LLG than vanilla SplitNN by offering more mixed intermediate gradients. In Li et al. (2021), the authors showed that a small KL divergences between the intermediate gradients from two classes could upper bound the maximal amount of label information the attacker can steal via LLG.

Proposition 3.1. *Let \tilde{P}^1 and \tilde{P}^0 be any perturbed distributions for intermediate gradients from class 1 and 0, and are continuous with respect to each other. For $\epsilon \in [0, 4)$,*

$$\begin{aligned} \text{KL}(\tilde{P}^1 \| \tilde{P}^0) + \text{KL}(\tilde{P}^0 \| \tilde{P}^1) &\leq \epsilon \\ \text{implies } \max_r \text{AUC}_r &\leq \frac{1}{2} + \frac{\sqrt{\epsilon}}{2} - \frac{\epsilon}{8}, \end{aligned} \quad (7)$$

where r is any LLG attack, and AUC_r represents the achieved AUC using r .

The proposition 3.1 indicates if the GAFM model outputs more mixed intermediate gradients from the two classes, it is more likely to offer better protection against different types of label-stealing attacks compared to vanilla SplitNN. Fig.2 shows the intermediate gradients using different methods on the Spam database. Comparing Fig.2 A and Fig.2 D1, GAFM has more mixed gradients than that from Vanilla SplitNN. Fig.2 D2 and Fig.2 D3 show the gradients from L_{GAN} and $L_{penalty}$ where the differences between gradient centers from the two classes have opposite direction, thus leading to the gradients cancellation in GAFM. We provide heuristic justification for the above-mentioned phenomena in Appendix A.

3.3 Choice of model parameters

GAFM has three model parameters σ , γ and Δ . As we mentioned earlier, the additive noise $\varepsilon \sim N(0, \sigma)$ is only introduced to make the reference (response) distribution have continuous support, and σ is considered small. Our

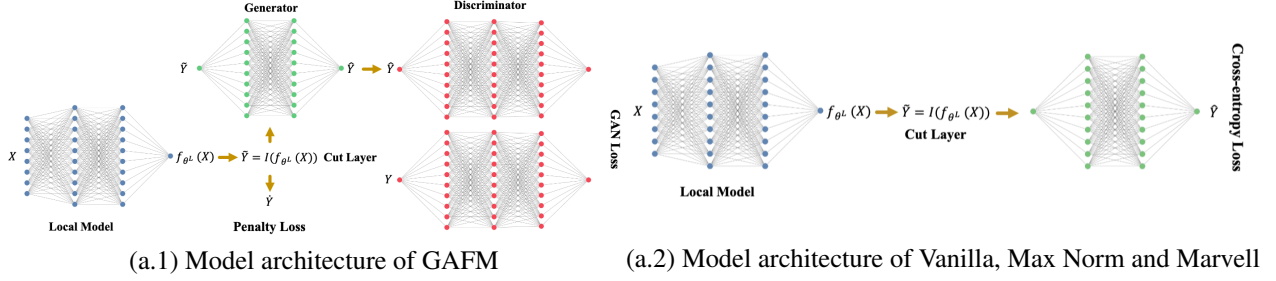


Figure 3: Experimental Model Architecture of Generative Adversarial Federated Model.

default choice is $\sigma = 0.01$, and we found the results to be insensitive to a wide range of $\sigma \in [0.01, 1]$ (see Appendix C.1).

Tuning γ can be difficult in GAFM if using unnormalized gradients when the GAN loss has gradients vanishing problem partly due to the weight clipping operation suggested by Wasserstein-based GAN (Arjovsky et al., 2017; Gulrajani et al., 2017). To address this, we have introduced the normalization operation at line 9 in Algorithm 1, defined as

$$f_{Norm}(X) = \frac{X}{\|X\|_2}. \quad (8)$$

The normalization operation alleviates the vanishing gradient problem and makes the GAN gradients and penalty gradients at the same scale. After this normalization, we fix $\gamma = 1.0$ as our default choice. Although a fixed γ may not be ideal, we achieved stably good performance across different numerical experiments given that we chose a reasonable Δ , which will be discussed in Section 4.2 and Appendix C.2.

3.4 Label stealing attacks

This section discusses three attack methods by which the attacker can steal label information from intermediate gradients in the binary classification task.

Norm Attack. Norm attack (Li et al., 2021) means norm-based attack which is a simple heuristic for black-box attack. It can be used for label inference in binary classification tasks. Norm attack is based on the observation that, for binary classification, the gradient norm $\|g\|_2$ of the positive instances tend to be different from that of the negative instances, especially with unbalanced datasets. Thus the gradient norm $\|g\|_2$ can be a strong predictor for labels.

Mean Attack. Mean-based attack is also a simple heuristic for black-box attack. In Li et al. (2021), the authors point out that the gradients from vanilla SplitNN tend to have a clustering structure with one class containing negative gradients and the other containing positive gradients. In GAFM, this sign relationship does not necessarily hold anymore. However, we can still try to make attacks based on which cluster a sample is closer to. We assume that the attackers know the gradient centers of class 0 and class 1, which are denoted as μ_0 and μ_1 . Let g_i be the intermediate gradient for sample i . The mean attacks assign the sample i to the cluster that g_i is closer to:

$$\hat{y}_i = \begin{cases} 1, & \text{if } \|g_i - \mu_1\|_2 \leq \|g_i - \mu_0\|_2 \\ 0, & \text{else.} \end{cases} \quad (9)$$

Median Attack. Median-based attack is similar as the mean attack. We consider the median attack because the median value is more robust to outliers than the mean value. Assuming that attackers know the gradient median of class 0 m_0 and class 1 m_1 and denote g_i as the intermediate gradient for sample i . The median attacks assign the sample i to the cluster that g_i is closer to:

$$\hat{y}_i = \begin{cases} 1, & \text{if } \|g_i - m_1\|_2 \leq \|g_i - m_0\|_2 \\ 0, & \text{else.} \end{cases} \quad (10)$$

4 Experiments

In this section, experiments are conducted to demonstrate the performance and security of GAFM. We first introduce datasets used in experiment and describe the experiment setup, including the model architecture, baselines, and evaluation metrics. We then report the experiment results in terms of performance, security and ablation study to show the superiority of GAFM and the contribution of each component of GAFM.

4.1 Datasets

We evaluate GAFM on three publicly available datasets.

Spambase dataset² collects 4061 emails with 57 attributes and they are classified as whether they are spam or not. And the proportion of positive instances is around 40%.

Credit dataset³ contains 24 attributes and 30000 instances of credit card clients such as default payments, demographic factors and payment history. The labels for the Credit dataset is a binary variable which shows whether the client is at risk of default. And the proportion of positive instances is around 22%.

IMDB dataset⁴ is a binary sentiment classification dataset containing 50000 highly polar movie reviews, of which 50% are positive and 50% are negative. The IMDB dataset has been preprocessed, and each review is encoded as a list of word indexes. We counted the top 500 frequent words in IMDB to construct the dataset used for the experiment.

Spambase, Credit and IMDB datasets have different degrees of imbalance and dimensionality, which allow us to evaluate the model in different label distribution scenarios and in high dimensions. More details of dataset processing are provided in Appendix D.1.

4.2 Experiment Setup

Model Architecture We consider the two-party setting with only one passive party in the main paper to focus on the label protection. More specifically, the active party only has the label information while the one passive party has all feature data without labels. In the section B.2, we also report the performance and security under multi-client (#clients=3) setting. The local model $f_{\theta_p^L}$ of the p th passive party, discriminator D_{θ^d} and generator G_{θ^g} for the active party are all simple multiple-hidden layer neural networks with different activation functions:

- G_{θ^g} : a two-hidden layer neural network with the Sigmoid activation function for the last layer and LeakyRelu activation function for the other layers.
- D_{θ^d} : a three-hidden hidden layer neural network with the LeakyRelu activation function for each layers.
- $f_{\theta_p^L}$: a two-hidden layer neural network with the Sigmoid activation function for the last layer and LeakyRelu activation function for the other layers.

We define the transformation function $F(\cdot)$ as the identity function $I(\cdot)$. More details are shown in Fig.3. We pick up the data-dependent parameter $\Delta = 0.05$ for Spambase, $\Delta = 0.1$ for both Credit and IMDB. We determine Δ based on the procedure described in Appendix C.2. For all datasets, we carry out our numerical experiments with parameters $\sigma = 0.01$, $\gamma = 1$, the clip value $c = 0.1$, the batch size $B = 1028$, the learning rate $\alpha^d = \alpha^L = \alpha^g = 1e - 4$ with Adam optimizer and the training epoch $T = 300$. Appendix D.2 provides more training details.

Baselines We compare the performance and security of GAFM with Marvell, Max Norm and vanilla SplitNN on the three public datasets.

Evaluation Metrics We use the Area Under Curve (AUC) to evaluate the model performance and use the leak AUC and Total Variation Distance (TVD) to measure the label leakage. We don't consider the differential privacy as the leakage measure since differential privacy is inapplicable to example-aware and example-specific setting like VFL Li et al. (2021).

Leak AUC. The leak AUC is defined as the AUC achieved using the defined attacks, e.g., norm attack or mean attack. When the leak AUC is close to 1, it implies that the attacker can very accurately recover the private label, whereas a small leak AUC around 0.5 indicates that the attacker is less informative in predicting the labels. In our experiments, to

²<https://archive.ics.uci.edu/ml/datasets/spambase>

³<https://www.kaggle.com/datasets/uciml/default-of-credit-card-clients-dataset>

⁴<http://ai.stanford.edu/~amaas/data/sentiment>

Table 1: Average AUC, Leak AUC and TVD using different models.

DATASET	METHOD	TRAIN	TEST	NORM ATTACK	MEAN ATTACK	MEDIAN ATTACK	TVD
SPAMBASE	GAFM	0.94±0.01	0.93±0.02	0.56±0.04	0.67±0.05	0.66±0.05	0.42±0.09
	MARVELL	0.71±0.09	0.71±0.08	0.53±0.02	0.70±0.01	0.70±0.01	0.39±0.07
	MAX NORM	0.95±0.00	0.95±0.00	0.83±0.11	1.00±0.00	0.91±0.00	0.97±0.05
	VANILLA	0.96±0.00	0.95±0.01	0.85±0.07	1.00±0.00	0.91±0.00	0.96±0.04
CREDIT	GAFM	0.65±0.07	0.65±0.07	0.61±0.06	0.63±0.11	0.63±0.10	0.31±0.20
	MARVELL	0.59±0.04	0.60±0.04	0.55±0.03	0.69±0.01	0.68±0.00	0.33±0.05
	MAX NORM	0.75±0.01	0.75±0.01	0.92±0.04	1.00±0.00	0.82±0.00	0.99±0.00
	VANILLA	0.75±0.01	0.74±0.01	0.95±0.01	1.00±0.00	0.82±0.00	0.99±0.00
IMDB	GAFM	0.92±0.02	0.90±0.01	0.55±0.06	0.67±0.02	0.67±0.02	0.36±0.06
	MARVELL	0.75±0.09	0.75±0.09	0.51±0.01	0.70±0.01	0.70±0.01	0.36±0.01
	MAX NORM	0.92±0.00	0.91±0.00	0.56±0.05	1.00±0.00	0.99±0.00	0.98±0.03
	VANILLA	0.92±0.00	0.91±0.00	0.62±0.05	1.00±0.00	0.99±0.00	0.98±0.00

account for the possibility that a simple label flipping may lead to higher leak AUC, we modify the leak AUC for a predefined attack as the following,

$$\text{leakAUC} \leftarrow \max(\text{leakAUC}, 1 - \text{leakAUC}) \quad (11)$$

That is, we flip our label assignment if this leads to higher AUC, and the resulting leak AUC is guaranteed to be no smaller than 0.5. Leak AUC have been widely used as a metric for measuring label leakage in previous work (Li et al., 2021; Yang et al., 2022; Sun et al., 2022).

Total Variation Distance. In order to guarantee that GAFM can defend against unknown attacks, we also introduce TVD as a privacy leakage measure. TVD measures the distance between a pair of probability measures (P, Q) which are defined on the same measurable space (Ω, \mathcal{F}) . It is

$$TV(P, Q) = \sup_{A \in \mathcal{F}} |P(A) - Q(A)|. \quad (12)$$

The smaller the TVD of the intermediate gradient distributions of different labels, the more difficult it is for the attacker to inference labels from the intermediate gradients.

4.3 Results

In this section, we report the classification AUC and different label leakage evaluation metrics. We also report results of ablation study. We run each method 10 runs with different random seeds and train-test splits. Details are shown in Appendix D

4.3.1 Evaluation of Prediction accuracy

Table 1 shows the achieved average AUC for different methods on the Spambase, Credit and IMDB datasets. The detailed distributions of leak AUC across 10 repetitions are shown in the Appendix B.3. GAFM achieves comparable classification AUC to Vanilla and Max Norm on all datasets, and is much higher than Marvell. Marvell experiences a performance loss due to perturbing the intermediate gradients with Gaussian noise.

4.3.2 Evaluation of Security

Next, we compare GAFM with baselines for label protection against different attacks. Table 1 shows the average leak AUC and average TVD. We see the Vanilla and Max Norm experience high leak AUC using norm, mean and median attacks. In contrast, GAFM and Marvell can protect against these attacks with leak AUC much closer to 0.5. GAFM is particularly good at protecting against mean and median attacks.

Further, the table 1 shows the results of average TVD, which provides conclusions consistent with that using leak AUC. The TVD of GAFM and Marvell are much smaller than Max Norm and Vanilla, implying that GAFM and Marvell have better protection against arbitrary unknown LLG attacks.

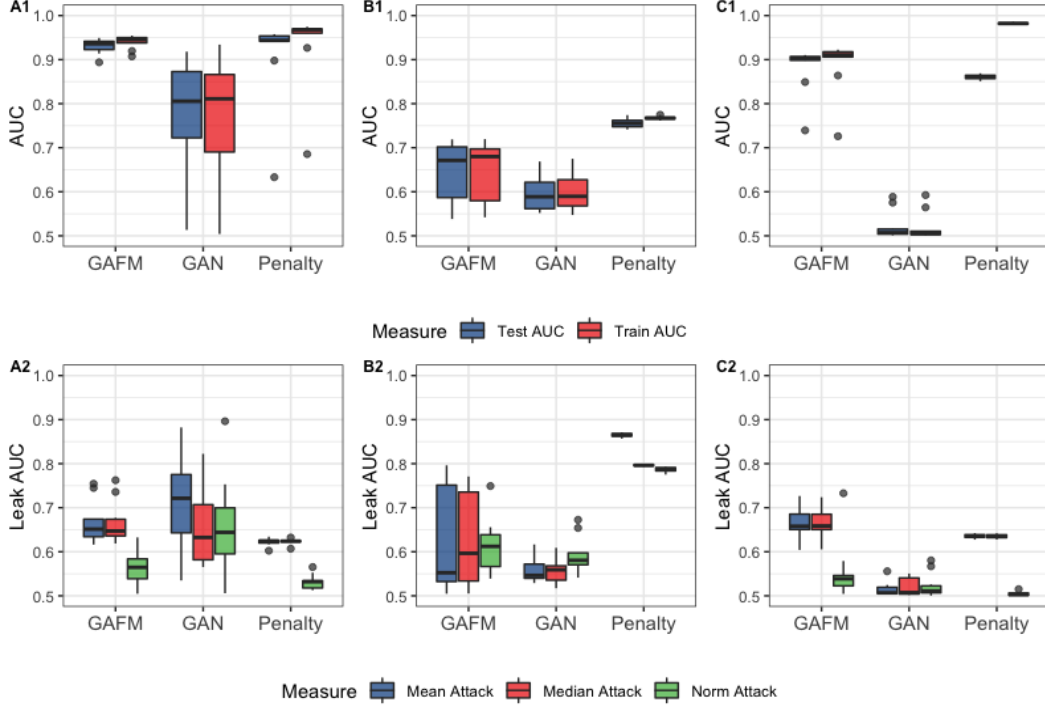


Figure 4: Fig 4A1 and Fig 4A2 are results on Spambase, Fig 4B1 and Fig 4B2 are on Credit and Fig 4C1 and Fig 4C2 are on IMDB. GAFM means GAFM with both GAN loss and penalty loss. GAN means GAFM with GAN loss only. Penalty means GAFM with penalty loss only.

Figure 2 shows the intermediate gradients from the cut layer using different models on the Spambase dataset in one repetition. Information on intermediate gradients using Credit and IMDB datasets are in Appendix B.1. The leak AUC achieves from different runs is shown in Appendix B.3.

4.3.3 Ablation Study

Fig.4 compares GAFM to the models with GAN loss only (referred to as GAN) and with penalty loss only (referred to as Penalty). We observe that GAFM sacrificed the prediction slightly for stable label privacy protection across different experiments. The Penalty model improves over the vanilla splitNN for label protection by using the randomized response \hat{Y} , and achieved low leak AUC when the resulting prediction model obtained high training AUC. However, in Credit dataset, the Penalty model has a median leak AUC as high as 0.8 across 10 repetitions with only around 0.1 increase in classification AUC compared to GAFM. Compared to GAN model which obtained low leak AUC in all three experiments, GAFM often achieved better classification AUC with the guidance from the penalty component: GAFM and Penalty models obtained leak AUC slightly higher than the GAN model in the IMDB dataset, but achieved classification AUC around 0.9 as opposed to around 0.5 using GAN model. Overall, GAFM achieved a robustly good trade-off between classification performance and security on different datasets by including both the GAN and the Penalty components.

5 Discussion

This paper presents the Generative Adversarial Federated Model (GAFM), which does not rely on complex encryption computing and can be applied to binary classification tasks under various vertical federated learning settings. Our empirical experiments demonstrated GAFM as a promising classification method with protection against LLG.

One popular way of guarding against LLG is to pass a noisy version of the intermediate gradients from the active party to passive parties, as in Marvell and Max Norm, which lead to better mixing of gradients from two classes in a binary classification problem. The GAFM takes a different path. By introducing the GAN loss and penalty loss into the learning task for the active party, we also observed improved gradient mixing compared to the vanilla SplitNN.

The goal of this paper is to introduce GAFM. Although we have considered a simple local model architecture in this paper, GAFM can utilize other local models for the passive parties. We also want to point out that GAFM and Marvell do not compete with each other. A nice property about Marvell is that it can guarantee the upper bound on label leakage from the gradients, while GAFM provides empirically good performance but is less rigorous. We can combine Marvell and GAFM by adding optimized random noise, which leads to automatic adaptation to the amount of mixing offered by GAFM, adding less random noise compared to vanilla Marvell when GAFM is doing well.

References

- Abadi, M., Chu, A., Goodfellow, I., McMahan, H. B., Mironov, I., Talwar, K., and Zhang, L. Deep learning with differential privacy. In *Proceedings of the 2016 ACM SIGSAC conference on computer and communications security*, pp. 308–318, 2016.
- Abuadbbba, S., Kim, K., Kim, M., Thapa, C., Camtepe, S. A., Gao, Y., Kim, H., and Nepal, S. Can we use split learning on 1d cnn models for privacy preserving training? In *Proceedings of the 15th ACM Asia Conference on Computer and Communications Security*, pp. 305–318, 2020.
- Aono, Y., Hayashi, T., Wang, L., Moriai, S., et al. Privacy-preserving deep learning via additively homomorphic encryption. *IEEE Transactions on Information Forensics and Security*, 13(5):1333–1345, 2017.
- Arjovsky, M., Chintala, S., and Bottou, L. Wasserstein generative adversarial networks. In Precup, D. and Teh, Y. W. (eds.), *Proceedings of the 34th International Conference on Machine Learning*, volume 70 of *Proceedings of Machine Learning Research*, pp. 214–223. PMLR, 06–11 Aug 2017. URL <https://proceedings.mlr.press/v70/arjovsky17a.html>.
- Ceballos, I., Sharma, V., Mugica, E., Singh, A., Roman, A., Vepakomma, P., and Raskar, R. Splitnn-driven vertical partitioning. *arXiv preprint arXiv:2008.04137*, 2020.
- Erdogan, E., Kupcu, A., and Cicek, A. E. Splitguard: Detecting and mitigating training-hijacking attacks in split learning. *arXiv preprint arXiv:2108.09052*, 2021.
- Frogner, C., Zhang, C., Mobahi, H., Araya, M., and Poggio, T. A. Learning with a wasserstein loss. *Advances in neural information processing systems*, 28, 2015.
- Geyer, R. C., Klein, T., and Nabi, M. Differentially private federated learning: A client level perspective. *arXiv preprint arXiv:1712.07557*, 2017.
- Goodfellow, I., Pouget-Abadie, J., Mirza, M., Xu, B., Warde-Farley, D., Ozair, S., Courville, A., and Bengio, Y. Generative adversarial nets. *Advances in neural information processing systems*, 27, 2014.
- Gulrajani, I., Ahmed, F., Arjovsky, M., Dumoulin, V., and Courville, A. C. Improved training of wasserstein gans. *Advances in neural information processing systems*, 30, 2017.
- Gupta, O. and Raskar, R. Distributed learning of deep neural network over multiple agents. *Journal of Network and Computer Applications*, 116:1–8, 2018.
- Ha, Y. J., Yoo, M., Lee, G., Jung, S., Choi, S. W., Kim, J., and Yoo, S. Spatio-temporal split learning for privacy-preserving medical platforms: Case studies with covid-19 ct, x-ray, and cholesterol data. *IEEE Access*, 9:121046–121059, 2021.
- Hardy, C., Le Merrer, E., and Sericola, B. Md-gan: Multi-discriminator generative adversarial networks for distributed datasets. In *2019 IEEE international parallel and distributed processing symposium (IPDPS)*, pp. 866–877. IEEE, 2019.
- Hardy, S., Henecka, W., Ivey-Law, H., Nock, R., Patrini, G., Smith, G., and Thorne, B. Private federated learning on vertically partitioned data via entity resolution and additively homomorphic encryption. *arXiv preprint arXiv:1711.10677*, 2017.
- Hitaj, B., Ateniese, G., and Perez-Cruz, F. Deep models under the gan: information leakage from collaborative deep learning. In *Proceedings of the 2017 ACM SIGSAC conference on computer and communications security*, pp. 603–618, 2017.
- Hu, R., Guo, Y., Li, H., Pei, Q., and Gong, Y. Personalized federated learning with differential privacy. *IEEE Internet of Things Journal*, 7(10):9530–9539, 2020.
- Li, O., Sun, J., Yang, X., Gao, W., Zhang, H., Xie, J., Smith, V., and Wang, C. Label leakage and protection in two-party split learning. *arXiv preprint arXiv:2102.08504*, 2021.
- Luo, X., Wu, Y., Xiao, X., and Ooi, B. C. Feature inference attack on model predictions in vertical federated learning. In *2021 IEEE 37th International Conference on Data Engineering (ICDE)*, pp. 181–192. IEEE, 2021.

- Mohassel, P. and Zhang, Y. Secureml: A system for scalable privacy-preserving machine learning. In *2017 IEEE symposium on security and privacy (SP)*, pp. 19–38. IEEE, 2017.
- Mugunthan, V., Gokul, V., Kagal, L., and Dubnov, S. Bias-free fedgan: A federated approach to generate bias-free datasets. *arXiv preprint arXiv:2103.09876*, 2021.
- Pardau, S. L. The california consumer privacy act: Towards a european-style privacy regime in the united states. *J. Tech. L. & Pol’y*, 23:68, 2018.
- Pereteanu, G.-L., Alansary, A., and Passerat-Palmbach, J. Split he: Fast secure inference combining split learning and homomorphic encryption. *arXiv preprint arXiv:2202.13351*, 2022.
- Poirot, M. G., Vepakomma, P., Chang, K., Kalpathy-Cramer, J., Gupta, R., and Raskar, R. Split learning for collaborative deep learning in healthcare. *arXiv preprint arXiv:1912.12115*, 2019.
- Rasouli, M., Sun, T., and Rajagopal, R. Fedgan: Federated generative adversarial networks for distributed data. *arXiv preprint arXiv:2006.07228*, 2020.
- Sun, J., Yang, X., Yao, Y., and Wang, C. Label leakage and protection from forward embedding in vertical federated learning. *arXiv preprint arXiv:2203.01451*, 2022.
- Titcombe, T., Hall, A. J., Papadopoulos, P., and Romanini, D. Practical defences against model inversion attacks for split neural networks. *arXiv preprint arXiv:2104.05743*, 2021.
- Vepakomma, P., Gupta, O., Swedish, T., and Raskar, R. Split learning for health: Distributed deep learning without sharing raw patient data. *arXiv preprint arXiv:1812.00564*, 2018.
- Voigt, P. and Von dem Bussche, A. The eu general data protection regulation (gdpr). *A Practical Guide, 1st Ed., Cham: Springer International Publishing*, 10(3152676):10–5555, 2017.
- Wainakh, A., Ventola, F., Müßig, T., Keim, J., Cordero, C. G., Zimmer, E., Grube, T., Kersting, K., and Mühlhäuser, M. User-level label leakage from gradients in federated learning. *Proceedings on Privacy Enhancing Technologies*, 2022 (2):227–244, 2022.
- Wang, Z., Song, M., Zhang, Z., Song, Y., Wang, Q., and Qi, H. Beyond inferring class representatives: User-level privacy leakage from federated learning. In *IEEE INFOCOM 2019-IEEE Conference on Computer Communications*, pp. 2512–2520. IEEE, 2019.
- Wu, Y., Kang, Y., Luo, J., He, Y., and Yang, Q. Fedcg: Leverage conditional gan for protecting privacy and maintaining competitive performance in federated learning. *arXiv preprint arXiv:2111.08211*, 2021.
- Yang, Q., Liu, Y., Cheng, Y., Kang, Y., Chen, T., and Yu, H. Federated learning. *Synthesis Lectures on Artificial Intelligence and Machine Learning*, 13(3):1–207, 2019.
- Yang, X., Sun, J., Yao, Y., Xie, J., and Wang, C. Differentially private label protection in split learning. *arXiv preprint arXiv:2203.02073*, 2022.
- Zhang, C., Li, S., Xia, J., Wang, W., Yan, F., and Liu, Y. {BatchCrypt}: Efficient homomorphic encryption for {Cross-Silo} federated learning. In *2020 USENIX Annual Technical Conference (USENIX ATC 20)*, pp. 493–506, 2020.
- Zhu, L., Liu, Z., and Han, S. Deep leakage from gradients. *Advances in Neural Information Processing Systems*, 32, 2019.

A Heuristic Justification for Improved Gradients Mixing

Here, we provide heuristic justification for why the GAN and penalty component in GAFM tends to have opposite direction.

- We assume that \tilde{Y} to be increase with Y since it tries to match \hat{Y} , which tends to increase with Y itself.

To optimize the equation (6), for the sample i , the intermediate gradient is:

$$\frac{\partial L_{GAFM}}{\partial \tilde{Y}_i} = \frac{\partial L_{GAN}}{\partial \tilde{Y}_i} + \gamma \frac{\partial L_{penalty}}{\partial \tilde{Y}_i}. \quad (A.1)$$

For the first term of equation (A.1):

$$\frac{\partial L_{GAN}}{\partial \tilde{Y}_i} = -\frac{\partial D_{\theta^d}(G_{\theta^g}(\tilde{Y}_i))}{N \partial \tilde{Y}_i} = -\frac{\partial D_{\theta^d}(\hat{Y}_i)}{N \partial \hat{Y}_i} \frac{\partial \hat{Y}_i}{\partial \tilde{Y}_i}. \quad (A.2)$$

- Consider the original GAN loss L_{GAN} and approximate it roughly with Taylor expansion:

$$\begin{aligned} L_{GAN}(\theta^d, \theta^g; \varepsilon) &= E[D_{\theta^d}(Y + \varepsilon)] - E[D_{\theta^d}(G_{\theta^g}(\tilde{Y}))] \\ &= E_{Y=1}[D_{\theta^d}(1 + \varepsilon) - D_{\theta^d}(\hat{Y})] + E_{Y=0}[D_{\theta^d}(\varepsilon) - D_{\theta^d}(\hat{Y})] \\ &\approx E_{Y=1}[\nabla D_{\theta^d}(1)(1 + \varepsilon - \hat{Y})] + E_{Y=0}[\nabla D_{\theta^d}(0)(\varepsilon - \hat{Y})] \\ &\approx E_{Y=1}[\nabla D_{\theta^d}(1)(1 - \hat{Y})] - E_{Y=0}[\nabla D_{\theta^d}(0)\hat{Y}]. \end{aligned}$$

Hence, $\nabla D_{\theta^d}(1)$ tends to be large and positive, and $\nabla D_{\theta^d}(0)$ tends to be small and negative. As a consequence, heuristically, $\nabla D_{\theta^d}(\hat{Y})$ tends to be positive and large if \hat{Y} is large, whereas $\nabla D_{\theta^d}(\hat{Y})$ tends to be small and negative if \hat{Y} is small.

- When \hat{Y} is increasing with Y , we tend to have (1) $\frac{\partial \hat{Y}}{\partial Y} > 0$, and (2) $\nabla D_{\theta^d}(\hat{Y}_1) - \nabla D_{\theta^d}(\hat{Y}_0) > 0$, where \hat{Y}_1, \hat{Y}_0 represent some \hat{Y} from class 1 and class 0 respectively. Hence, $\frac{\partial L_{GAN}}{\partial Y_1}$ tend to be smaller than $\frac{\partial L_{GAN}}{\partial Y_0}$ where \tilde{Y}_1, \tilde{Y}_0 represent some \tilde{Y} from class 1 and class 0. This is what we observed in FIG.2D2.
- When \hat{Y} is decreasing with Y , we tend to have (1) $\frac{\partial \hat{Y}}{\partial Y} < 0$, and (2) $\nabla D_{\theta^d}(\hat{Y}_1) - \nabla D_{\theta^d}(\hat{Y}_0) < 0$. Hence, we still have $\frac{\partial L_{GAN}}{\partial Y_1}$ tend to be smaller than $\frac{\partial L_{GAN}}{\partial Y_0}$. This is what we observed in FIG.B.1D2 and FIG.B.2D2.

Combining them together, the distribution of GAN gradients at $Y = 1$ tends to be left of the distribution at $Y = 0$.

For the second term of equation (A.1):

$$\frac{\partial L_{penalty}}{\partial \tilde{Y}_i} = \frac{1}{N} \left(-\frac{\dot{Y}}{\tilde{Y}_i} + \frac{1 - \dot{Y}}{1 - \tilde{Y}_i} \right) = \frac{1}{N} \frac{\tilde{Y}_i - \dot{Y}}{\tilde{Y}_i(1 - \tilde{Y}_i)}. \quad (A.3)$$

Without the GAN loss part, in a perfectly fitted model, we tend to have,

$$\begin{cases} E(\tilde{Y}_i|Y_i = 1) = E(\dot{Y}_i|Y_i = 1) = 0.5 + \frac{\Delta}{2} \\ E(\tilde{Y}_i|Y_i = 0) = E(\dot{Y}_i|Y_i = 0) = 0.5 - \frac{\Delta}{2} \end{cases}. \quad (A.4)$$

In practice, an imperfect fit tends to have $E(\tilde{Y}_i|Y_i = 1) < E(\dot{Y}_i|Y_i = 1)$ and $E(\tilde{Y}_i|Y_i = 0) > E(\dot{Y}_i|Y_i = 0)$. In addition, with the GAN loss part, the larger gradient (usually) for $Y = 0$ from the GAN loss drives \tilde{Y}_i to decrease more at $Y = 0$ compared to that from $Y = 1$. Combining them together, heuristically, we tend to have,

$$\frac{\partial L_{penalty}}{\partial \tilde{Y}_i} = \begin{cases} \frac{\tilde{Y}_i - \dot{Y}}{N \tilde{Y}_i(1 - \tilde{Y}_i)} > 0 & Y_i = 1 \\ \frac{\tilde{Y}_i - \dot{Y}}{N \tilde{Y}_i(1 - \tilde{Y}_i)} < 0 & Y_i = 0 \end{cases} \quad (A.5)$$

Penalty gradients at $Y = 1$ tend to be the right of the distribution at $Y = 0$. This is what we observe in Fig.2 D3, Fig.B.1 D3 and Fig.B.2 D3.

Finally, combining equations (A.2) and (A.5), the normalized final gradient for L_{GAFM} is

$$\frac{\partial L_{GAFM}}{\partial \hat{Y}_i} = \begin{cases} f_{Norm}(-\nabla D_{\theta^d}(\hat{Y}_i) \frac{\partial \hat{Y}_i}{\partial \hat{Y}_i}) \downarrow + \gamma f_{Norm}(\frac{\tilde{Y}_i - \hat{Y}_i}{N\hat{Y}_i(1-\hat{Y}_i)}) \uparrow & Y = 1 \\ f_{Norm}(-\nabla D_{\theta^d}(\hat{Y}_i) \frac{\partial \hat{Y}_i}{\partial \hat{Y}_i}) \uparrow + \gamma f_{Norm}(\frac{\tilde{Y}_i - \hat{Y}_i}{N\hat{Y}_i(1-\hat{Y}_i)}) \downarrow & Y = 0 \end{cases}, \quad (A.6)$$

where the normalization operation is $f_{Norm}(X) = \frac{X}{\|X\|_2}$ which does not change the order of gradients. This heuristic analysis suggests that the gradients from the GAN component and the penalty component tends to have opposite direction. Equation (A.6) demonstrates GAN loss gradient and penalty loss gradient help the total gradient to mix better by mutual perturbation.

B Additional Experiment Results

B.1 Intermediate gradients on Credit

Fig.B.1 and Fig.B.2 show the gradients on Credit and IMDB datasets. GAFM has much more mixed gradients compared with Vanilla and Max Norm. The mixed gradients of GAFM is caused by the cancellation between GAN loss gradients and penalty loss gradients.

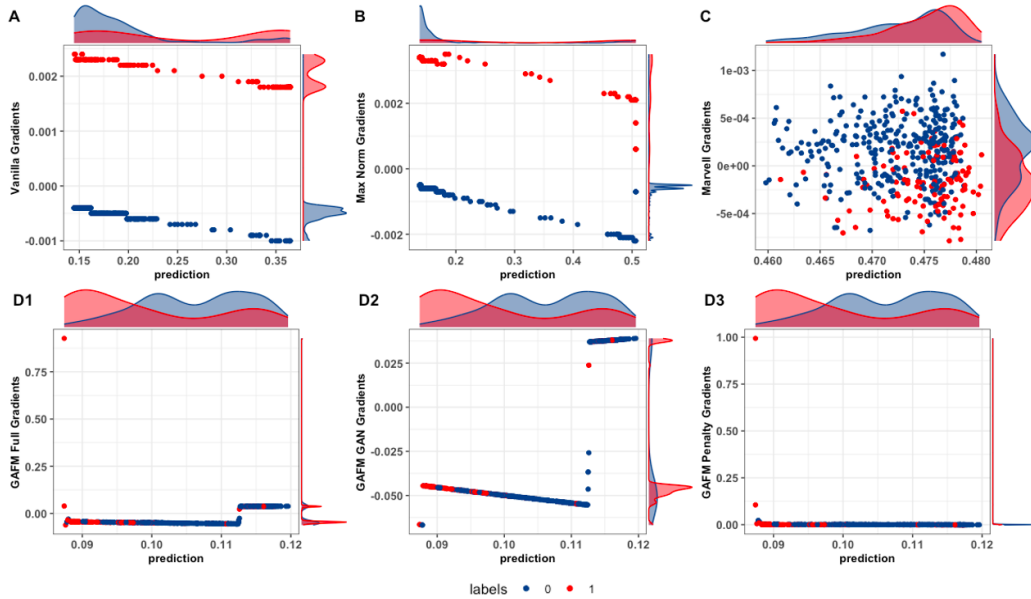
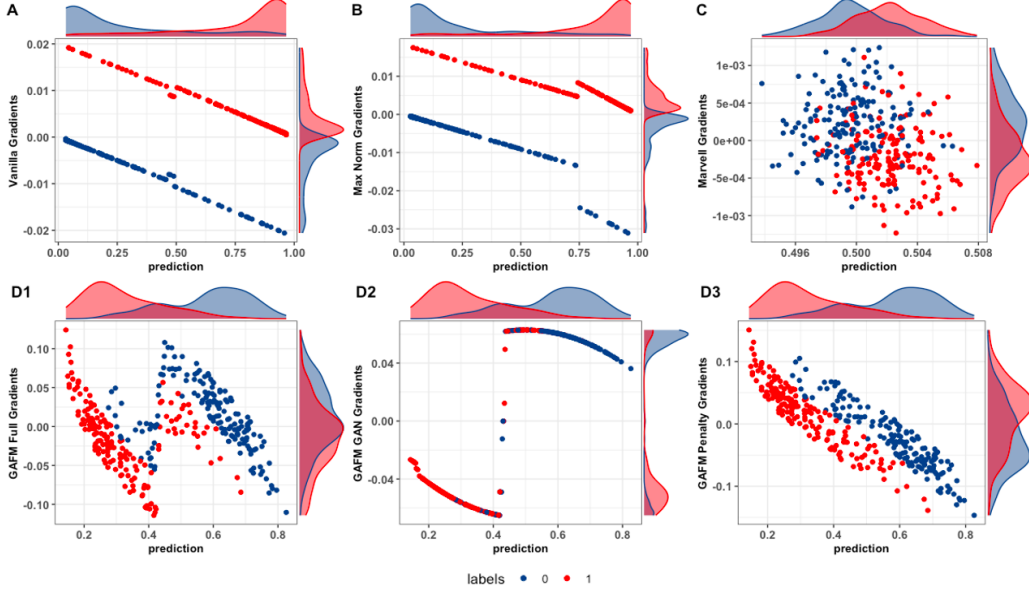


Figure B.1: Prediction \hat{Y} vs. Intermediate Gradients of different models on Credit.

Figure B.2: Prediction \hat{Y} vs. Intermediate Gradients of different models on IMDB.

B.2 Multiple Clients

In this section, we extend the two-party split learning to multi-party split learning. Assume that there are three passive parties and one active party jointly training GAFM. We split the training and test samples in the ratio of 7 : 3 and repeat each method 10 runs. The local feature assignment for the three participants is $client_1 : client_2 : client_3 = 19 : 19 : 19$ for Spambase, $client_1 : client_2 : client_3 = 8 : 8 : 7$ for Credit and $client_1 : client_2 : client_3 = 200 : 200 : 100$ for IMDB. The model architecture of the passive party's local model, generator and discriminator are identical to the model architecture in the section 4.2. The only difference is the transformation function $F(\cdot)$ is no longer the identity function $I(\cdot)$, but the averaging function

$$\tilde{y} = F(\tilde{y}_1, \tilde{y}_2, \tilde{y}_3) = \frac{\tilde{y}_1 + \tilde{y}_2 + \tilde{y}_3}{3}. \quad (\text{B.1})$$

Table B.1: Average AUC, Leak AUC and TVD using different models under multiple clients setting.

DATASET	METHOD	TRAIN	TEST	NORM ATTACK	MEAN ATTACK	MEDIAN ATTACK	TVD
SPAMBASE	GAFM	0.87±0.15	0.86±0.15	0.60±0.07	0.69±0.06	0.68±0.07	0.52±0.11
	MARVELL	0.70±0.05	0.68±0.06	0.53±0.03	0.70±0.02	0.70±0.02	0.37±0.05
	MAX NORM	0.95±0.00	0.95±0.00	0.83±0.11	0.99±0.02	0.99±0.04	0.94±0.08
	VANILLA	0.95±0.00	0.95±0.00	0.84±0.13	1.00±0.00	1.00±0.00	0.96±0.06
CREDIT	GAFM	0.71±0.02	0.70±0.02	0.71±0.06	0.80±0.03	0.76±0.03	0.60±0.05
	MARVELL	0.59±0.05	0.59±0.05	0.55±0.03	0.69±0.00	0.69±0.00	0.36±0.03
	MAX NORM	0.76±0.00	0.75±0.00	0.93±0.05	0.95±0.04	1.00±0.00	0.99±0.00
	VANILLA	0.75±0.00	0.75±0.00	0.96±0.02	0.97±0.03	1.00±0.00	0.99±0.00
IMDB	GAFM	0.88±0.01	0.87±0.01	0.52±0.01	0.65±0.03	0.65±0.03	0.30±0.05
	MARVELL	0.70±0.10	0.70±0.09	0.51±0.01	0.69±0.00	0.69±0.00	0.26±0.09
	MAX NORM	0.91±0.00	0.90±0.00	0.52±0.02	1.00±0.00	1.00±0.00	0.93±0.05
	VANILLA	0.91±0.00	0.90±0.00	0.52±0.01	1.00±0.00	1.00±0.00	0.98±0.05

Table B.1 shows the AUC, leak AUC and TVD results. Here, the leak AUC and TVD measure the leakage of all passive parties but also the leakage of each passive party since the \tilde{y}_1 , \tilde{y}_2 and \tilde{y}_3 are equally weighted as the cut layer. We

observe that the performance and security of both GAFM and Marvell slightly decrease in the multi-party setting compared to the two-party setting. It may be due to the fact that multiple participants setting makes jointly training more difficult. In the multi-client setting, GAFM still achieves the best trade-off between performance and security compared to all baselines.

B.3 Distribution of Leak AUC across repetitions

Fig.B.3 shows the leak AUC distribution of GAFM, Marvell, Max Norm and Vanilla against norm, mean and median attacks. We see GAFM is clustered in the bottom right in most of figures which illustrates the advantages of GAFM over Marvell, Max Norm and Vanilla in terms of prediction accuracy and privacy protection.

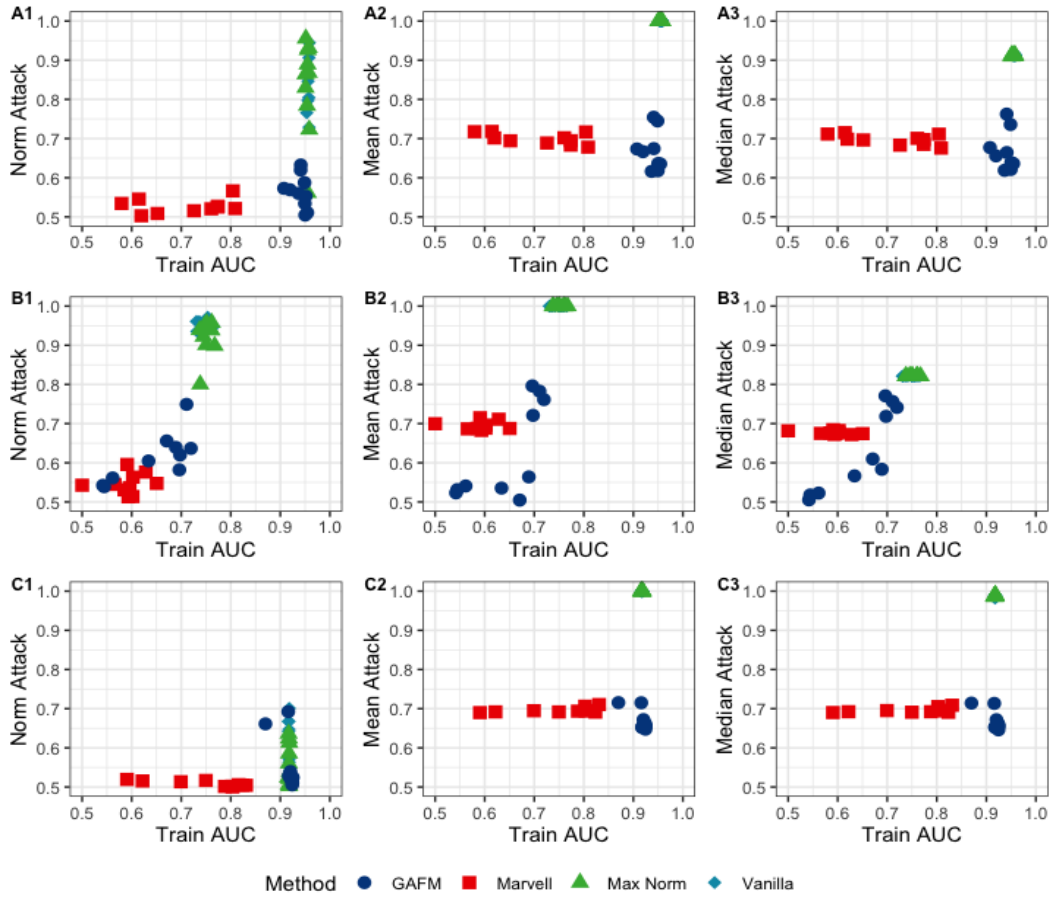


Figure B.3: Fig.B.3 A1-A3 are results on Spambase, Fig.B.3 B1-B3 are results on Credit and Fig.B.3 C1-C3 are results on IMDB.

C Discussion on model parameters

C.1 Discussion on σ

Comparing GAFM with different σ across 10 repetitions in Table C.1, we observe that a moderately large σ does not lead to severe deterioration in prediction accuracy and can provide almost the same robust protection against label stealing attacks.

Table C.1: Average AUC, Leak AUC and TVD using different models of different GAFM(σ).

DATASET	METHOD	TRAIN	TEST	NORM ATTACK	MEAN ATTACK	MEDIAN ATTACK	TVD
SPAMBASE	GAFM(0.01)	0.94 \pm 0.01	0.93 \pm 0.02	0.56 \pm 0.04	0.67 \pm 0.05	0.66 \pm 0.05	0.42 \pm 0.09
	GAFM(0.25)	0.94 \pm 0.01	0.93 \pm 0.01	0.60 \pm 0.06	0.67 \pm 0.03	0.67 \pm 0.03	0.42 \pm 0.05
	GAFM(1)	0.94 \pm 0.01	0.94 \pm 0.01	0.57 \pm 0.05	0.68 \pm 0.04	0.68 \pm 0.04	0.42 \pm 0.09
CREDIT	GAFM(0.01)	0.65 \pm 0.07	0.65 \pm 0.07	0.61 \pm 0.06	0.63 \pm 0.11	0.63 \pm 0.10	0.31 \pm 0.20
	GAFM(0.25)	0.67 \pm 0.03	0.66 \pm 0.03	0.57 \pm 0.06	0.69 \pm 0.10	0.68 \pm 0.08	0.40 \pm 0.19
	GAFM(1)	0.68 \pm 0.02	0.68 \pm 0.02	0.62 \pm 0.05	0.73 \pm 0.06	0.72 \pm 0.05	0.46 \pm 0.15
IMDB	GAFM(0.01)	0.92 \pm 0.02	0.90 \pm 0.01	0.55 \pm 0.06	0.67 \pm 0.02	0.67 \pm 0.02	0.36 \pm 0.06
	GAFM(0.25)	0.92 \pm 0.00	0.90 \pm 0.00	0.53 \pm 0.01	0.65 \pm 0.01	0.65 \pm 0.01	0.31 \pm 0.02
	GAFM(1)	0.92 \pm 0.00	0.90 \pm 0.00	0.53 \pm 0.02	0.65 \pm 0.02	0.64 \pm 0.02	0.30 \pm 0.05

C.2 Discussion about picking up Δ

We then discuss how to determine the data-dependent parameter Δ in GAFM. In the section 4.2, we pick up the Δ based on the measure $Ratio = \frac{leakAUC}{trainAUC}$ and the minimum average ratio criteria. It means we consider the Δ which has the minimum average ratio of all attacks. Also, we want the training AUC on the subset to be at least the threshold τ to guarantee the prediction accuracy of GAFM. So the optimal Δ^* on the subset can be written as the solution of following equations,

$$\begin{aligned} & \min Ratio_{\Delta} \\ & \text{s.t. } trainAUC_{\Delta} \geq \tau \end{aligned} \quad (C.1)$$

In our experiment, we set the threshold τ to 0.6 and the values of Δ are in $[0.05, 0.1, 0.2, 0.3, 0.5]$.

The detailed procedure is as follows. For privacy purposes, we only sample a small portion (10%) of the dataset without replacing to be shared between the active and passive parties and train GAFM on this small subset to determine the appropriate Δ across 5 repetitions. Then, we average the ratio of norm attack, mean attack and median attack for different Δ in the table C.2. And based on ratio and τ , we pick up the optimal Δ^* for subset Spambase is 0.05 with the average training AUC equals to 0.93, the optimal Δ^* for subset Credit is 0.1 with the average training AUC equals to 0.64 and the optimal Δ^* for subset IMDB is 0.1 with the average training AUC equals to 0.61.

Table C.2: Average ratio of norm attack, mean attack and median attack on full data and subset.

DATASET	SAMPLING RATIO	$\Delta = 0.05$	$\Delta = 0.1$	$\Delta = 0.2$	$\Delta = 0.3$	$\Delta = 0.5$
SPAMBASE	1	0.699	0.717	0.707	0.755	0.824
	0.1	0.673	0.768	0.864	0.902	0.931
CREDIT	1	0.910	0.896	0.941	0.962	1.099
	0.1	1.013	1.216	1.219	1.410	1.434
IMDB	1	0.945	0.791	0.898	01.023	0.876
	0.1	0.964	1.135	1.256	1.234	1.359

Fig.C.1 further shows the detailed ratio distribution on the full dataset and the small subset. We see along with the increase in Δ , almost all the ratio of each attack increases for these two datasets. And the Δ marked by the green shading (on the full dataset) is identical to the Δ marked by the red shading (on the sampling dataset) besides the Δ on Spambase. Fig.C.1 illustrates that it is feasible to determine the Δ by the minimum average ratio criteria on small sampling subset.

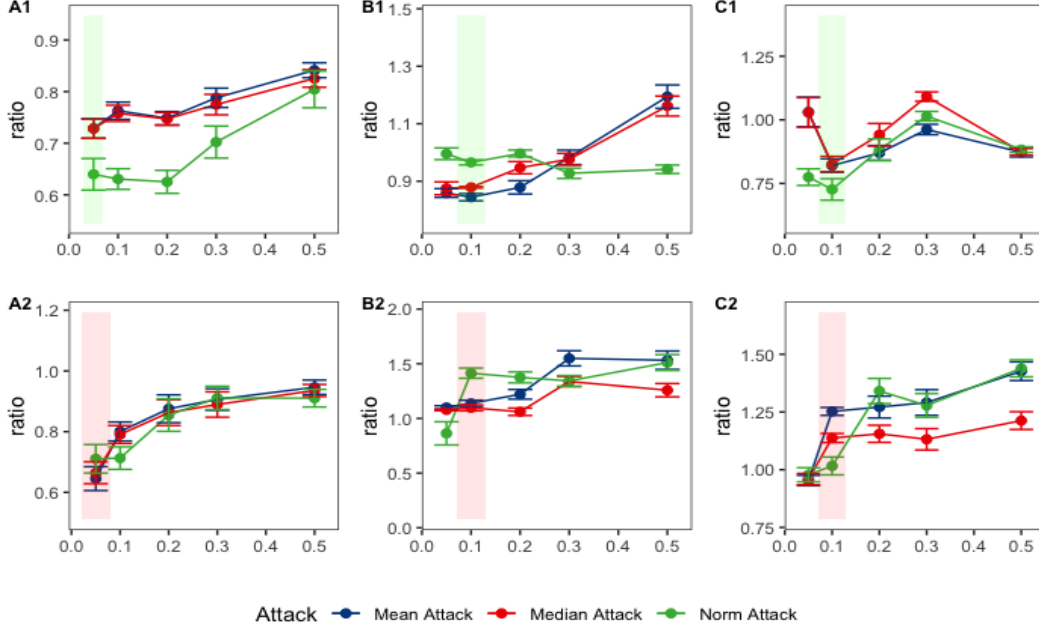


Figure C.1: Fig.C.1 A1-A2 are results on Spambase, Fig.C.1 B1-B2 are results on Credit and Fig.C.1 C1-C2 are results on IMDB. The first row in Fig.C.1 shows the ratio on full dataset where the optimal Δ is marked by the green shade. The second row in Fig.C.1 shows the ratio on subset with sampling ratio equals to 0.1 where the optimal Δ is marked by the red shade. We repeat GAFM 5 runs on each dataset with different random seeds and average them to estimate the AUC and leak AUC to reduce variance.

D Data setup and Experiment Details

In this section, we first describe how we pre-process the three public datasets in D.1. Then, we describe what the training hyperparameters for each dataset/model combination in D.2.

D.1 Dataset Processing

Spambase There are 4061 instances in the dataset. Each instance of Spambase data has 55 continuous real attributes and 2 continuous integer attributes. We first replace all the NA values in the data with 0 and then normalize features to reduce the effect of magnitudes. At each repetition, we further make the dataset into a 70%-30% train-test split at different random seed settings.

Credit The Credit dataset has 30000 instances and 24 features. We first remove the ID, the feature used for identification. Then, we replace all NA value with a single new category (the empty string) for each categorical feature and replace all NA value with 0 for each real-valued feature and then normalize features to reduce the effect of magnitudes. Similarly, at each repetition, we further make the dataset into a 70%-30% train-test split at different random seed settings.

IMDB The IMDB data has been preprocessed and words are encoded as a sequence of word indexes in the form of integers. We select the top 500 words and encode indexes with one-hot. The 50000 reviews are split into 25000 for training and 25000 for testing at different random seeds. And the final training and test data are both 25000×500 matrices filled with 0s and 1s.

D.2 Model Training Details

Spambase, Credit and IMDB We consider mini-Batch Learning strategy with batch size equals to 1028 for training. For all model components, we use Adam optimizer with a learning rate of $1e-4$ and set training epoch $T = 300$, clip value $c = 0.1$. We train both GAFM and baseline models 10 times each and set the seeds from 0 to 9. The initial \hat{Y} at the first epoch is generated from the standard Gaussian distribution $\mathcal{N}(0, 1)$. We conduct our experiments on PyTorch and CPU. Each run of Spambase takes about 10 minutes to finish, each run of Credit takes about 1 hour to finish and each run of IMDB takes about 1.1 hour to finish.